論文の内容の要旨

In Vitro and In Vivo Delivery of Drugs and siRNA Mediated by Water-Soluble Fullerenes

(水溶性フラーレンを用いた薬剤および siRNA の in vitro，in vivo 輸送)

南　皓輔

1. Introduction

Nanomaterials have gained much attention as their potential applications in the fields of material and biological sciences. Especially in the field of biomedical applications, development of drug delivery systems is a challenging work since improving drug efficacy and reducing side effects of drugs. Research efforts are focused on designing drug carriers, which effectively deliver into cells. For the carriers controlling the size in the range of several tens of nanometer to submicrometer and their surface functionalities are important subjects. Water-soluble fullerene derivatives form nano- to micrometer-sized aggregates and show unique structures in water due to the high hydrophobicity of fullerene backbones. Construction of well-controlled aggregated structures of fullerenes and their surface functionalities enables us to utilize them for biomedical applications. In this Ph. D. thesis, I have developed the fullerene-based nanomaterials and applied them for drug and gene delivery systems.

2. Cationic fullerene as a carrier of siRNA delivery

RNA interference (RNAi) has emerged as one of the most powerful tools for a sequence specific suppression of gene expressions. The key mediator of RNAi is small interfering RNA (siRNA), which is non-coding RNA with 21 to 23 nucleotide-length. siRNA has low stability under

physiological environment due to the degradation by nuclease, and high solubility in water, so it is difficult to deliver and pass through the hydrophobic cell membranes. Therefore, the effective carriers are required. I focused on a cationic fullerene derivative TPFE (Chart 1). TPFE has cationic piperazines, which interact with polyanionic RNA backbone by electrostatic interaction, and fullerene core, which shows the hydrophobic nature to aggregate in water. Thus, I expected that TPFE formed globules with siRNA in water to stabilize and deliver into cells.

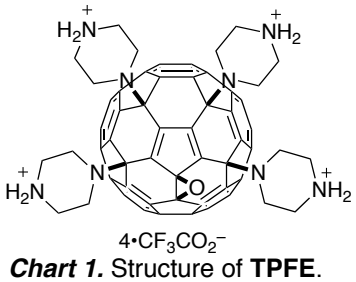

Chart 1. Structure of **TPFE**.

I mixed TPFE with siRNA in the range of reagent-to-base pair (*R*) ratio from 0 to 50, and formation of globules and their sizes were determined by electrophoresis and DLS, respectively (Figure 1). Although the *R* values from 0 to 10 obtained precipitates with the size over 1 μm and free siRNA on the electrophoresis, the *R* value of 20 showed submicrometer-sized globules and disappearance of free siRNA, suggesting the completion of the globule formation.

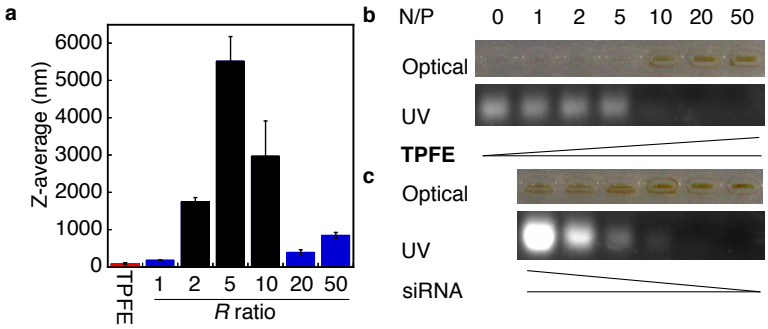

Figure 1. Formation of **TPFE**-siRNA globules. (a) DLS measurement of the globules. (b), (c) N/P ratio-dependent agarose-gel electrophoresis of the globules with different dose of (b) **TPFE** and (c) siRNA.

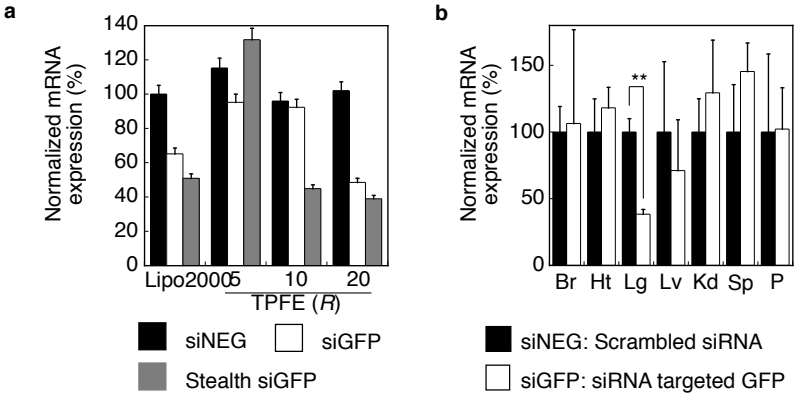

Figure 2. siRNA delivery in vitro and in vivo. (a) siRNA delivery in vitro. (b) siRNA delivery in vivo. $^{**}P < 0.005$.

The TPFE was mixed with siRNA targeting GFP (siGFP) and incubated together with GFP-overexpressed human embryonic kidney (GFP-HEK) cells for 48 h. The RNAi efficiency was determined by quantitative real-time RT-PCR (qRT) as the expression level of mRNA (Figure 5a). The highest knockdown was observed at the *R* value of 20. In addition, TPFE showed higher knockdown efficiency than Lipofectamine2000, a commercially available and widely studied lipid-based siRNA delivery agent. Finally, I studied in vivo siRNA delivery using GFP-expressed mice. I intravenously injected TPFE-siRNA solution ($R = 20$) into mice, sacrificed the mice after 24 h and collected tissue specimens. The RNAi efficiency was determined by qRT (Figure 5b). The GFP expression level on lung showed 62% knockdown, whereas the other tissues obtained no significant differences. In addition, TPFE did not show any cytotoxicity within the experimental dose. TPFE shows lung-selective delivery, which indicates utility of TPFE as RNAi therapy for the lung diseases.

3. Characterization of post-functionalizable fullerene vesicle and its application for drug delivery

I succeeded in developing a post-functionalizable fullerene vesicle **C8(7Y)K** via Cu(I)-catalyzed click reactions (Figure 3). **C8(7Y)K** vesicle exposes terminal alkynes to its surface derived from the unique amphiphilic molecule **C8(7Y)K**, which features a nonpolar/polar/nonpolar ternary motif, and the alkynes react with azide compounds with retaining its vesicular structure. Considering the installation of functionalities on the surface of the vesicle as well as the high stability towards chemical reactions, I have expected that the installation of bioactive molecules on the surface would afford the vesicle where the surface was densely covered with proteins.

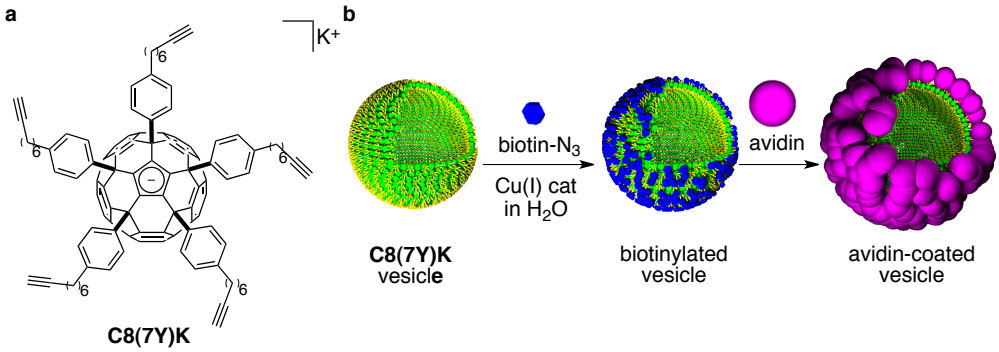

Figure 3. Post-functionalizable fullerene vesicle **C8(7Y)K**. (a) Structure of **C8(7Y)K**. (b) Schematic illustration of post-functionalization and protein modification.

For this purpose, I introduced azido-biotin onto the surface of **C8(7Y)K** vesicle to obtain biotinylated **C8(7Y)K** vesicle (Figure 3). The biotinylated vesicle retained a spherical structure with an average diameter of 23 nm determined by dynamic light scattering (DLS) and scanning electron microscopy (SEM) (Figure 4a and d). When I mixed the biotinylated **C8(7Y)K** vesicle with avidin in PBS, the diameter of the vesicle increased 7.7 nm determined by SEM, which corresponds to the size of avidin (Figure 2b and d). During the SEM study, after irradiation with accumulated electron dose, some of the avidin-coated vesicle showed fine structures (Figure 4c and d). The average area of the dents was 30–45 and 65–75 nm^2, which corresponds to the one and two avidin molecules, respectively. These results indicate that the biotinylated **C8(7Y)K** vesicle were fully covered with avidin.

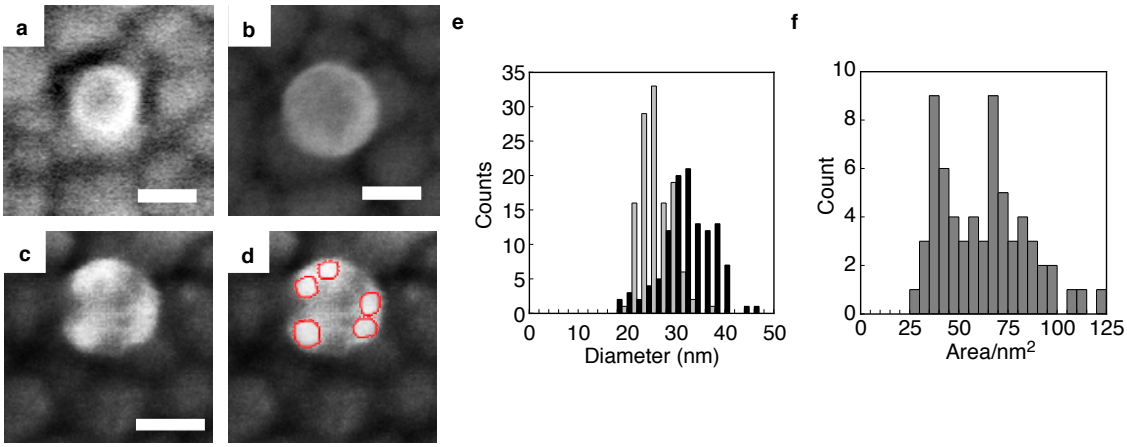

Figure 4. SEM images of biotinylated **C8(7Y)K** vesicles. SEM images of (a) biotinylated vesicle, (b) avidin-coated vesicle and (c) avidin-coated vesicle with fine structures. Scale bars: 20 nm. (d) The vesicle in Figure 2c, where bright areas are highlighted in red. (e) Histogram of size of vesicles. Gray and black bars indicate biotinylated vesicle and avidin-coated vesicle, respectively. (f) Histogram of area of fine structures.

The biotinylated **C8(7Y)K** vesicle shows the biomolecular recognition by avidin as described above. In addition, the vesicle has the hollow space with the diameter of ca. 30 nm, and can entrap water-soluble molecules. I expected that the biotinylated **C8(7Y)K** vesicle can be applicable for the vehicle of drugs to deliver its cargo into cells. Thus, I prepared **C8(7Y)K** vesicle in the presence of anticancer drug, doxorubicin (DOX), put the biotin moieties by click reaction, and separated from the vesicle with excess DOX and unreacted azido-biotin by gel permeation chromatography.

I incubated this vesicle solution together with human liver carcinoma (HepG2) cells for 48 h. The 2.5 pmol of free DOX (25 nM as the final concentration) did not show any cytotoxicity, whereas the vesicle entrapping 2.5 pmol of DOX showed 25% cytotoxicity (Figure 3). Thus, the DOX entrapped in the vesicle was effectively delivered into the cells, released in the cytoplasm and killed the cancer cells at a total dose much lower than the treatment of free DOX (IC_{50} value of free DOX was 3.4 μM).

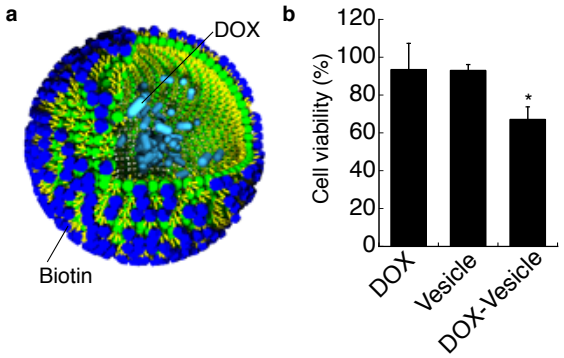

Figure 5. Doxorubicin delivery. (a) Schematic image of DOX-encapsulated biotinylated vesicle (DOX-vesicle). (b) Cell viability of HepG2 cells. $^{*}P < 0.05$.

4. Conclusion

I have developed water-soluble fullerene-based nanomaterials for application of drug and siRNA delivery. In drug delivery, extremely low amount of anticancer drug delivered by **C8(7Y)K** vesicle showed significant antitumor activity in vitro. In siRNA delivery, cationic fullerene TPFE showed RNAi efficiency both in vitro and in vivo. In addition, both fullerene derivatives, **C8(7Y)K** and TPFE has no cytotoxicity. The results described here suggested that water-soluble fullerene derivatives would give us an insight of designing carriers for drug delivery systems.